JOURNAL OF Materials CHEMISTRY

Stability properties and phase relations of $Fe^{3+}_{4-x}Fe^{2+}_{3x}(PO_4)_3(OH)_{3-3x}O_{3x}$ in the quaternary system $FeO–Fe_2O_3–P_2O_5–H_2O$

Peter Schmid-Beurmann*

Institut für Geowissenschaften, Christian Albrechts Universität Kiel, D-24098 Kiel, Germany. E-mail: psb@min.uni-kiel.de

Received 31st July 2000, Accepted 11th October 2000
First published as an Advance Article on the web 8th January 2001

The phase relations in the quaternary system $FeO–Fe_2O_3–P_2O_5–H_2O$ were investigated under hydrothermal conditions at 386 and 586 °C at a pressure of 0.3 GPa. Under these conditions a restricted solid solution series coexists with the H_2O bearing fluid phase between the $Fe_2(PO_4)O$ and $Fe_4(PO_4)_3(OH)_3$ compositions. The members of this solid solution series were found to be isotypic to tetragonal β-$Fe_2(PO_4)O$. At 586 °C the composition of this series covers the range between $0.18 \leqslant x \leqslant 0.60$ according to a stoichiometry of $Fe^{3+}_{4-x}Fe^{2+}_{3x}(PO_4)_3(OH)_{3-3x}O_{3x}$. With decreasing temperature this compositional range is reduced to compositions between $0.52 \leqslant x \leqslant 0.58$. At 586 °C the $Fe_2(PO_4)O_{ss}$ solid solution series was found to coexist with hematite (Fe_2O_3), sarcopside ($Fe_3(PO_4)_2$), $Fe_7(PO_4)_6$ and monoclinic $Fe_4(PO_4)_3(OH)_3$ whereas at 386 °C they coexist with α-Fe_2O_3 (hematite), $Fe_3(PO_4)_2$ (sarcopside), $Fe_7(PO_4)_6$ and $Fe_3(PO_4)_2(OH)_2$ (barbosalite). The synthesis runs with the same compositions and *P–T* conditions but different starting compounds yielded a nearly phase pure member of the $Fe_2(PO_4)O_{ss}$ solid solution series. Therefore these results support the assumption that the $Fe_2(PO_4)O_{ss}$ solid solution is a stable product under the applied hydrothermal conditions.

Introduction

Mixed valent Fe-phosphates of the β-$Fe_2(PO_4)O$ structure type have gained some attention in the last decade because of their crystal, chemical and catalytic properties. This structure can be regarded as built up of layers of parallel chains of face-sharing oxygen octahedra. Between alternating layers the chains are approximately perpendicular to each other and they are interconnected *via* PO_4-tetrahedra and common oxygen or hydroxyl ions (Fig. 1).

Tetragonal β-$Fe_2(PO_4)O$ is the first mixed valence compound in which iron with a mean oxidation number of 2.5 has been observed in a single crystallographic site located at the center of face-sharing octahedra.[1] Therefore the situation is looked upon to be ideal for theoretical treatments due to the especially short Fe–Fe distance of 2.67 Å.

On the other hand the hydroxy phosphates like Fe^{2+}-$Fe^{3+}_2(OH)_2(PO_4)_2$ as well as $Fe_{4.24}(PO_4)_3(OH)_{2.28}O_{0.72}$ with the same structural framework as β-$Fe_2(PO_4)O$ but different Fe-occupancy and OH-content, have gained some attention as catalysts for the oxidative dehydrogenation of isobutyric acid (IBA) to methacrylic acid (MAA).[2,3] As a result of catalytic studies on different iron hydroxy phosphates these authors reported that synthetic barbosalite and synthetic lipscombite, both $Fe^{2+}Fe^{3+}_2(OH)_2(PO_4)_2$, as well as $Fe_{4.24}(PO_4)_3(OH)_{2.28}O_{0.72}$ and $Fe_5(PO_4)_3O_3$ changed their compositions during the catalytic process resulting in three members of a possible solid solution series between β-$Fe^{2+}Fe^{3+}(PO_4)O$ and $Fe^{3+}_4(OH)_3(PO_4)_3$ with the ideal formula of $Fe^{3+}_{4-x}Fe^{2+}_{3x}(PO_4)_3(OH)_{3-3x}O_{3x}$. Recently it was shown that a restricted solid solution series exists between the β-$Fe^{2+}Fe^{3+}(PO_4)O$ and $Fe^{3+}_4(OH)_3(PO_4)_3$ compositions under hydrothermal conditions.[4] This paper now focuses on the thermal evolution of the solid solution and the phase relations in the quaternary system $FeO–Fe_2O_3–P_2O_5–H_2O$.

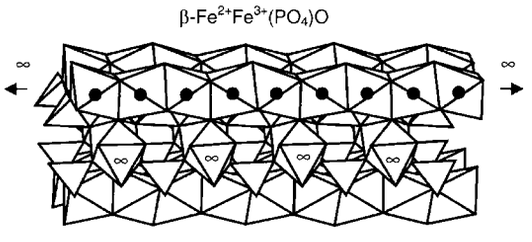

Fig. 1 Structure of tetragonal β-$Fe_2(PO_4)O$.[1] Black circles: Fe with intermediate valency. This structure type can be regarded as built up of infinite chains of face-sharing oxygen octahedra which are interconnected *via* PO_4-tetrahedra and common oxygen or hydroxyl ions. The face-sharing octahedra are fully occupied (designed after Rouzies and Millet).[26]

Previous work

The phase relations in the anhydrous system $FeO–Fe_2O_3–P_2O_5$ were intensively studied in synthesis experiments under dry conditions in evacuated quartz ampoules (Fig. 2).[5] As ternary phosphates in this system the compounds $Fe_2(PO_4)O$, $Fe_7(PO_4)_6$, $Fe_9(PO_4)O_8$, $Fe_5(PO_4)_3O$, $Fe_3(P_2O_7)_2$ and $Fe_7(P_2O_7)_4$ appear. Among these there are $Fe_7(PO_4)_6$, $Fe_5(PO_4)_3O$ as well as Fe_2O_3 (hematite) which were found to coexist with the α-modification of $Fe_2(PO_4)O$. The latter undergoes two phase transitions according to the sequence:[1,6,7]

$$\beta(\text{mcl}) \Rightarrow 142^{\circ}\text{C} \Rightarrow \beta(\text{tet}) \Rightarrow 700-800^{\circ}\text{C} \Rightarrow \alpha(\text{orth})$$

The high temperature modification α-$Fe_2(PO_4)O$ was synthesised in evacuated quartz ampoules from mixtures of (Fe_2O_3, $FePO_4$, Fe), ($Fe_2P_2O_7$, Fe_2O_3) or [Fe_3PO_7, $Fe_3(PO_4)_2$].[8]

 DOI: 10.1039/b006566h

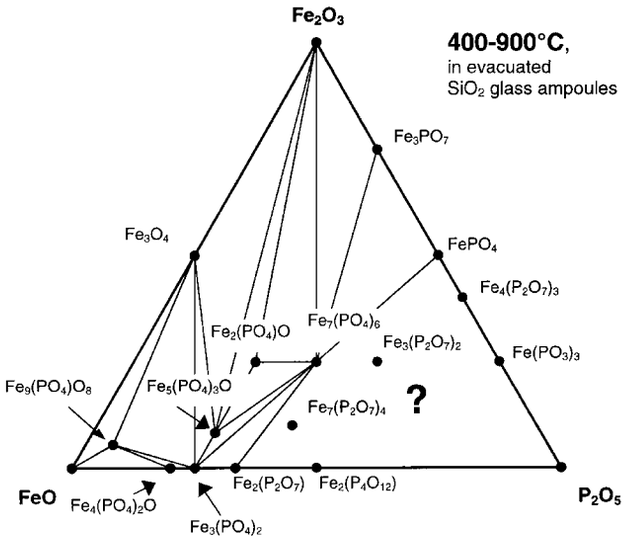

Fig. 2 Anhydrous phases in the ternary system FeO–Fe_2O_3–P_2O_5.[5]

The low temperature modification β-$Fe_2(PO_4)O$ was prepared by evaporation of an aqueous solution of $Fe(NO_3)_3$ and $(NH_4)_2HPO_4$ or H_3PO_4 at temperatures up to 400 °C and subsequent reduction in a H_2–H_2O gas atmosphere diluted with N_2 at 450 °C.[6] The attempted synthesis of β-$Fe_2(PO_4)O$ by other methods *e.g.* chemical vapour transport with $FeCl_2$ or HCl, hydrothermal synthesis at 0.4 GPa and 600 °C or high pressure synthesis (5 GPa, 600 °C) yielded the α-modification or other phases which were not fully characterised.[1] These results lead to the assumption that β-$Fe_2(PO_4)O$ has a limited stability range and begins to transform to the α-modification at 600 or 700 °C under vacuum.[1,6] The monoclinic distortion of β-(mcl)-$Fe_2(PO_4)O$ below 142 °C was detected by using synchroton powder diffraction.[7]

The compound $Fe_7(PO_4)_6$ was first synthesised hydrothermally in Cu-ampoules at temperatures between 250 and 450 °C and a pressure of about 0.1 GPa.[9] Later it was reported as a crystallisation product of Fe-phosphate glasses at 800 °C.[10] $Fe_5(PO_4)_3O$ was first synthesised from mixtures of Fe_3PO_7 and $Fe_3(PO_4)_2$ in evacuated silica tubes.[11]

The addition of H_2O to the system FeO–Fe_2O_3–P_2O_5 leads to a multitude of phases (Fig. 3) of which only the compounds with less water content like $Fe^{2+}(OH)(PO_4)$, wolfeite, the monoclinic title compound $Fe_4(OH)_3(PO_4)_3$ as well as $Fe_3(OH)_2(PO_4)_2$ (lipscombite and barbosalite) are supposed to be stable at elevated temperatures. $Fe_4(OH)_3(PO_4)_3$ was first synthesised using the hydrothermal method at temperatures of about 400 °C.[12,13]

Recently a restricted solid solution series was synthesised at 600 °C and 0.3 GPa between $Fe^{2+}Fe^{3+}PO_4O$ and $Fe_4^{3+}(OH)_3(PO_4)_3$. These compounds were found to be isotypic to tetragonal β-$Fe_2(PO_4)O$ using standard X-ray diffraction techniques.[4] The composition of this solid solution series was found to cover the range within $0.18 \leqslant x \leqslant 0.60$ according to the ideal formula of $Fe^{3+}_{4-x}Fe^{2+}_{3x}(PO_4)_3(OH)_{3-3x}O_{3x}$ previously proposed for these compounds.[3]

Experimental

Synthesis

The phase relations of the solid solution series between $Fe_2(PO_4)O$ and $Fe_4(PO_4)_3(OH)_3$ (denoted as $Fe_2(PO_4)O_{ss}$) in the quaternary system FeO–Fe_2O_3–P_2O_5–H_2O were studied in hydrothermal synthesis runs. As starting materials, Fe (Merck no. 819 p.a.), Fe_2O_3 (Merck no. 3924), $FePO_4$ (berlinite form), $Fe_7(PO_4)_6$, $Fe_3(PO_4)_2$, α-Fe_2PO_4O and $Fe_4(PO_4)_3(OH)_3$ were used. $FePO_4$ was synthesised from pelletised stoichiometric mixtures of Fe_2O_3 and $(NH_4)H_2PO_4$ (Fluka no. 09709) by successive heatings in an open platinum crucible between 350 and 1000 °C. After regrinding the product was again pelletised and then fired in an open silica tube at 1000 °C for three days. The phase characterisation using X-ray powder diffraction revealed single phase $FePO_4$ with the berlinite (α-$AlPO_4$) structure. $Fe_3(PO_4)_2$ (graftonite), α-Fe_2PO_4O and $Fe_7(PO_4)_6$ were synthesised from pelletised stoichiometric mixtures of Fe, Fe_2O_3 and $FePO_4$ by heating at 900 °C in evacuated silica tubes over periods of up to 3 days.[8,14] $Fe_4(PO_4)_3(OH)_3$ was prepared hydrothermally over three days from $FePO_4$ and Fe_2O_3 at 450 °C.[13]

The starting compounds were weighed in the appropriate proportions and homogenised in a mortar. 100 mg of the material was sealed into Au tubes with a length of 30 mm, an outer diameter of 3 mm and a wall thickness of 0.1 mm together with an excess of distilled water. All the experiments were carried out in a conventional hydrothermal apparatus with horizontally arranged Tuttle-type cold-seal bombs at temperatures of 386 and 586 °C at a pressure of 0.3 GPa. The temperature was controlled using Ni–CrNi thermocouples with an estimated overall uncertainty of less than ±5 °C. The pressure was measured with a Heise gauge with an uncertainty

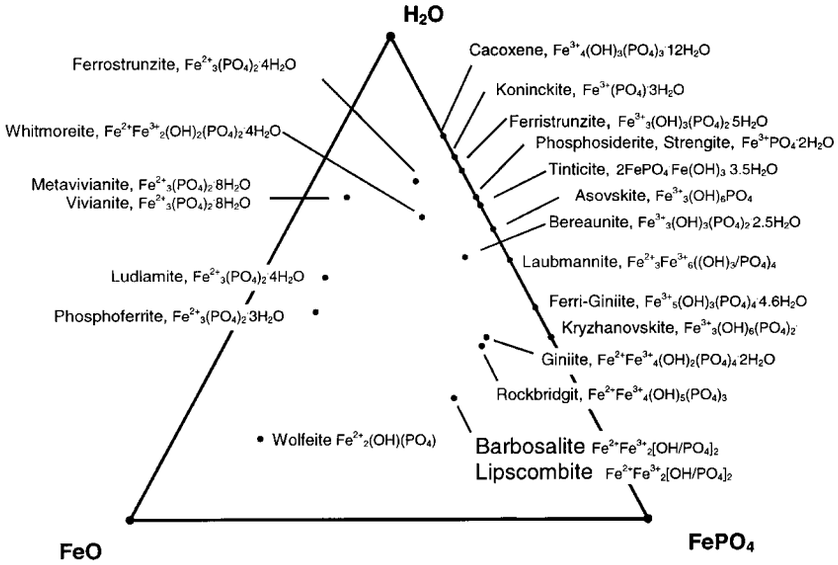

Fig. 3 Hydrous mineral phases in the quaternary system FeO–Fe_2O_3–P_2O_5–H_2O projected onto the pseudo ternary section FeO–$FePO_4$–H_2O.[27]

of ± 2.5 MPa. The experiments were ended by switching off the power. The autoclaves were then cooled to room temperature within half an hour in a cold air stream .

X-Ray powder diffraction

X-Ray powder diffractograms for qualitative and quantitative phase analysis of the run products were recorded using a SIEMENS D5000 with Cu-Kα radiation and a secondary graphite (001) monochromator with the operation conditions $U = 40$ kV and $I = 30$ mA. The phases present in the samples were identified using the standards from the JCPD-ICCD database with the help of the Siemens DIFFRAC-AT[28] software package. Quantitative phase analysis and determination of the lattice constants was performed using the Rietveld program HILL.[15] The samples were ground in an agate mortar and 30–40 mg of the powder was transferred onto glass sample holders, and smoothed by a microscopy glass substrate giving layers with a 15×12 mm surface and about 0.1 mm thickness. The weight portions of the crystalline phases present in the run products were determined using multiphase Rietveld refinement of the X-ray powder diffractograms. The structural data of $Fe_4(PO_4)_3(OH)_3$,[12] β-$Fe_2(PO_4)O$,[1] hematite,[16] sarcopside,[17] $Fe_7(PO_4)_6$,[9] and $Mg_3(PO_4)_2(OH)_2$ (for the isotypic compound $Fe_3(PO_4)_2(OH)_2$, barbosalite)[18] were taken as starting parameters for the identified phases. Diffraction data from 17 to 70° (2θ) were included in the calculation.

Determination of the composition of $Fe_2(PO_4)O_{ss}$

The composition of the members of the $Fe_2(PO_4)O_{ss}$ present in the run products was determined *via* a calibration curve according to the expression:

$$V/\text{Å}^3 = 349.1(2) + 11.2(4)x \quad (1)$$

This calibration curve is based on the dependency of their tetragonal unit cell volume V on composition in the range of the solid solution between $Fe_2(PO_4)O$ and $Fe_4(PO_4)_3(OH)_3$.[4] This function is valid in the compositional range of the intermediate solid solution series between $0.18 \leqslant x \leqslant 0.60$.

Results

Optical characterisation of the run products

The hydrothermal experiments resulted in black fine grained powders. Optical inspection using a microscope revealed that the members of the $Fe_2(PO_4)O_{ss}$ series were present in the form of isometric crystals showing faces with rounded edges. These individual crystals had diameters up to 10 μm and were opaque in transmitted light. $Fe_3(PO_4)_2(OH)_2$ (barbosalite) forms irregular crystals with dimensions up to 10 μm which were transparent and showed dark green absorption in transmitted light. $Fe_3(PO_4)_2$ (sarcopside) could easily be recognised when present in the samples as it forms yellowish transparent crystals with well developed faces and dimensions of about 100 μm. The compound $Fe_7(PO_4)_6$ was detected in several samples and formed black single crystals showing crystal faces and dimensions up to 100 μm.

Phase analysis

The experimental conditions and the results of the synthesis runs performed at 586 and 386 °C in the phase diagram FeO–P_2O_5–Fe_2O_3–H_2O are presented in Tables 1 and 2, respectively. The chemical bulk composition of the anhydrous starting material of the runs are given as molar fractions of the oxides FeO, P_2O_5 and Fe_2O_3 (columns 2–4). If the bulk composition of a sample is located on the pseudo binary section between the $Fe_2(PO_4)O$ and $Fe_4(PO_4)_3(OH)_3$ composition additionally the compositional parameter x is given (column 5). This parameter x is related to the ideal chemical formula of $Fe^{3+}_{4-x}Fe^{2+}_{3x}(PO_4)_3(OH)_{3-3x}O_{3x}$ proposed by Rouzies *et al.*[3] for members of the $Fe_2(PO_4)O_{ss}$ solid solution series. The last column of Tables 1 and 2 give the results of the qualitative and quantitative phase analysis of the run products. The weight percentages of the detected phases as determined by multiphase Rietveld refinement are given in parentheses. In Table 3 the results of synthesis runs with the same bulk composition *but* different starting materials are listed.

In Table 4 the lattice constants, the unit cell volume and the compositional parameter x of members of the $Fe_2PO_4O_{ss}$ solid solution series present in the products of the synthesis runs are given. The compositional parameters x which refer to the formula $Fe^{3+}_{4-x}Fe^{2+}_{3x}(PO_4)_3(OH)_{3-3x}O_{3x}$ were calculated from eqn. (1).

Phase relations at 586 °C

In Fig. 4a the phase relations of the $Fe_2(PO_4)O_{ss}$ solid solution series at 586 °C, which were derived from the experimental runs of Table 1, are shown as a projection to the ternary system FeO–Fe_2O_3–P_2O_5 from the H_2O apex. Under water saturated conditions the $Fe_2(PO_4)O_{ss}$ solid solution series was found to coexist with α-Fe_2O_3 (hematite), $Fe_3(PO_4)_2$ (sarcopside), $Fe_7(PO_4)_6$ and the limiting member of a solid solution near to the $Fe_4(PO_4)_3(OH)_3$ composition. The tieline between $Fe_2(PO_4)O_{ss}$ and the latter phase is dotted in Fig. 4a. The diagonal crosses ($\times$) represent the starting compositions of the runs from Table 1 (columns 2–4) whereas in the section on the left hand side of the diagram the vertical crosses (+) mark the compositions of the $Fe_2(PO_4)O_{ss}$ solid solution members according to their compositional parameter x (Table 4).

Table 1 Synthesis experiments at 586 °C and 0.3 GPa

	Starting bulk composition					
Barb-	$x_{Fe_2O_3}$[a]	x_{FeO}[a]	$x_{P_2O_5}$[a]	x[b]	t/days	Phase composition of the products
35	0.250	0.500	0.250	1.000	4	$Fe_2(PO_4)O_{ss}$ (84), Hem (1), Sarc (15)
60	0.286	0.444	0.270	0.824	2	$Fe_2(PO_4)O_{ss}$ (94), Hem (3), Sarc (3)
56	0.323	0.387	0.290	0.667	2	$Fe_2(PO_4)O_{ss}$ (98), Hem (2)
57	0.361	0.328	0.311	0.526	2	$Fe_2(PO_4)O_{ss}$ (97), Hem (3)
54	0.400	0.267	0.333	0.400	2	$Fe_2(PO_4)O_{ss}$ (99), Hem (1)
58	0.441	0.203	0.356	0.286	2	$Fe_2(PO_4)O_{ss}$ (97), Hem (3)
133[d]	0.526	0.070	0.404	0.087	1	$Fe_2(PO_4)O_{ss}$ (57), $Fe_4(PO_4)_3(OH)_3$ (43)
49	0.571	0.000	0.429	0.000	2	$Fe_4(PO_4)_3(OH)_3$ (100)
59[c]	0.526	0.070	0.404	0.875	2	$Fe_2(PO_4)O_{ss}$ (91), $Fe_7(PO_4)_6$ (9)
77[c]	0.361	0.328	0.311	0.375	2	$Fe_2(PO_4)O_{ss}$ (79), $Fe_7(PO_4)_6$ (13), Sarc(9)

Starting materials: Fe, Fe_2O_3 and $FePO_4$. Abbreviations used: Barb: barbosalite $Fe_3(PO_4)_2(OH)_2$, Hem: hematite (α-Fe_2O_3), Sarc: sarcopside [$Fe_3(PO_4)_2$]. [a]Molar fractions in the ternary system FeO–Fe_2O_3–P_2O_5. [b]Compositional parameter x according to the formula $Fe^{3+}_{4-x}Fe^{2+}_{3x}(PO_4)_3(OH)_{3-x}$. [c]Broken sample container which affected strong reduction of the sample due to direct contact with the pressure medium which led to the formation of $Fe_7(PO_4)_6$. [d]Sample weight 450 mg in an Au-container with an outer diameter of 5 mm.

Table 2 Synthesis experiments at 386 °C and 0.3 GPa

Barb-	Starting bulk composition				*t*/days	Phase composition of the products
	$x_{Fe_2O_3}$[a]	x_{FeO}[a]	$x_{P_2O_5}$[a]	x[b]		
88	0.250	0.500	0.250	1.000	3	$Fe_2(PO_4)O_{ss}$ (69), Hem (8), Sarc (23)
81	0.286	0.444	0.270	0.824	3	$Fe_2(PO_4)O_{ss}$ (96), Hem (4)
82	0.323	0.387	0.290	0.667	3	$Fe_2(PO_4)O_{ss}$ (97), Hem (3)
105	0.341	0.358	0.301	0.597	3	Barb (63), $Fe_2(PO_4)O_{ss}$ (33), Hem (3)
83	0.361	0.328	0.311	0.526	3	Barbosalite (94), Hem (6)
84	0.400	0.267	0.333	0.400	3	Barb (74), $Fe_4(PO_4)_3(OH)_3$ (22), Hem (4)
85	0.441	0.203	0.356	0.286	3	Barb (59), $Fe_4(PO_4)_3(OH)_3$ (39), Hem (2)
86	0.483	0.138	0.379	0.182	3	Barb (33), $Fe_4(PO_4)_3(OH)_3$ (66), Hem (1)
87	0.526	0.070	0.404	0.087	3	Barb (23), $Fe_4(PO_4)_3(OH)_3$ (76), Hem (1)
48	0.571	0.000	0.429	0.000	2	$Fe_4(PO_4)_3(OH)_3$
106	0.371	0.253	0.376	—	3	Barb (60), $Fe_7(PO_4)_6$ (10), $Fe_4(PO_4)_3(OH)_3$ (29)
107	0.274	0.423	0.304	—	3	Barb (61), Sarc (7), $Fe_2(PO_4)O_{ss}$ (32)
108	0.162	0.421	0.416	—	3	Barb (55), Sarc (44)
14	0.333	0.333	0.333	—	5	Barb (100)

Starting materials: Fe, Fe_2O_3 and $FePO_4$. Abbreviations used: Barb: barbosalite $Fe_3(PO_4)_2(OH)_2$, Hem: hematite (α-Fe_2O_3), Sarc: sarcopside [$Fe_3(PO_4)_2$]. [a]Molar fractions in the ternary system FeO–Fe_2O_3–P_2O_5. [b]Compositional parameter x according to the formula $Fe^{3+}_{4-x}Fe^{2+}_{3x}(PO_4)_3(OH)_{3-3x}O_{3x}$.

Table 3 Synthesis experiments with different starting materials at 586 °C and 0.3 GPa

Barb-	x[a]	Starting materials	t[b]/days	Run products
113	0.286	$Fe_7(PO_4)O_6$, α-Fe_2O_3, $FePO_4$	3	$Fe_2(PO_4)O_{ss}$
58	0.286	$FePO_4$, α-Fe_2O_3, α-Fe	2	$Fe_2(PO_4)O_{ss,}$ (hematite, $FePO_4$)
72	0.286	α-$Fe_2(PO_4)O$, $Fe_4(PO_4)_3(OH)_3$	2	$Fe_2(PO_4)O_{ss}$
116	0.286	$Fe_3(PO_4)_2$, α-Fe_2O_3, $FePO_4$	2	$Fe_2(PO_4)O_{ss}$

[a]Compositional parameter x of the starting mixture according to the formula of $Fe^{3+}_{4-x}Fe^{2+}_{3x}(PO_4)_3(OH)_{3-3x}O_{3x}$. [b]$t$, duration of the experiment. Container material: Au-ampoules with a length of 30 mm, a diameter of 3 mm and a wall thickness of 0.1 mm.

Table 4 Compositions from lattice constants

Barb-	Lattice constants of tetragonal $Fe_2(PO_4)O_{ss}$[a]			
	a/Å	b/Å	V/Å^3	x[b]
Samples synthesised at 586 °C				
35	5.3053(6)	12.662(2)	356.4(1)	0.65(4)
77	5.2705(3)	12.815(1)	355.98(5)	0.61(2)
60	5.2940(2)	12.7004(6)	355.94(3)	0.61(2)
57	5.2686(2)	12.8002(7)	355.31(1)	0.55(2)
56	5.2565(3)	12.831(1)	354.54(4)	0.49(2)
54	5.2451(2)	12.8400(7)	353.24(3)	0.37(2)
116	5.2370(9)	12.871(3)	353.0(2)	0.34(3)
72	5.2220(2)	12.9215(7)	352.36(3)	0.29(2)
113	5.2288(4)	12.883(1)	352.23(6)	0.28(2)
58	5.2198(2)	12.917(1)	351.94(4)	0.25(2)
59	5.2114(2)	12.9461(7)	351.60(3)	0.22(2)
Samples synthesised at 386 °C				
81	5.2773(4)	12.769(1)	355.62(6)	0.58(2)
88	5.2793(6)	12.747(2)	355.3(1)	0.55(2)
107	5.266(2)	12.804(7)	355.1(3)	0.54(4)
82	5.2691(7)	12.787(2)	355.0(1)	0.53(2)
105	5.266(1)	12.797(5)	354.9(1)	0.52(2)

[a]Setting of the unit cell according to the space group $I4_1/amd$.[1] [b]Compositional parameter x according to the formula $Fe^{3+}_{4-x}Fe^{2+}_{3x}(PO_4)_3(OH)_{3-3x}O_{3x}$ calculated from the calibration function of eqn. (1).

The phase relations in the binary section [$Fe_2(PO_4)O_{ss}$, $Fe_7(PO_4)_6$] and in the ternary [$Fe_2(PO_4)O_{ss}$, $Fe_7(PO_4)_6$] were derived from synthesis runs in which the Au-container was broken and the sample material came into direct contact with the reducing H_2O-pressure medium (Barb-59 and -77). The oxygen fugacity of the latter is determined by the steel of the autoclave which is comparable to the reducing Ni/NiO-buffer.[19] Therefore the bulk compositions of these runs (Barb-59 and Barb-77) were shifted within the reaction period of one day along the arrows in Fig. 4 due to a reduction to lower Fe^{3+}-contents entering the [$Fe_2(PO_4)O_{ss}$, $Fe_7(PO_4)_6$] (Barb-59) and [$Fe_2(PO_4)O_{ss}$ + $Fe_7(PO_4)_6$ + sarcopside] field (Barb-77).

Phase relations at 386 °C

The phase relations at 386 °C are presented in Fig. 4b. The starting compositions of the corresponding runs are shown as diagonal crosses ($\times$). Under these conditions a solid solution between $Fe_2(PO_4)O$ and $Fe_4(PO_4)_3(OH)_3$ is formed only in the small range between $0.52 \leqslant x \leqslant 0.58$ according to a stoichiometry of $Fe^{3+}_{4-x}Fe^{2+}_{3x}(PO_4)_3(OH)_{3-3x}O_{3x}$. The positions of the

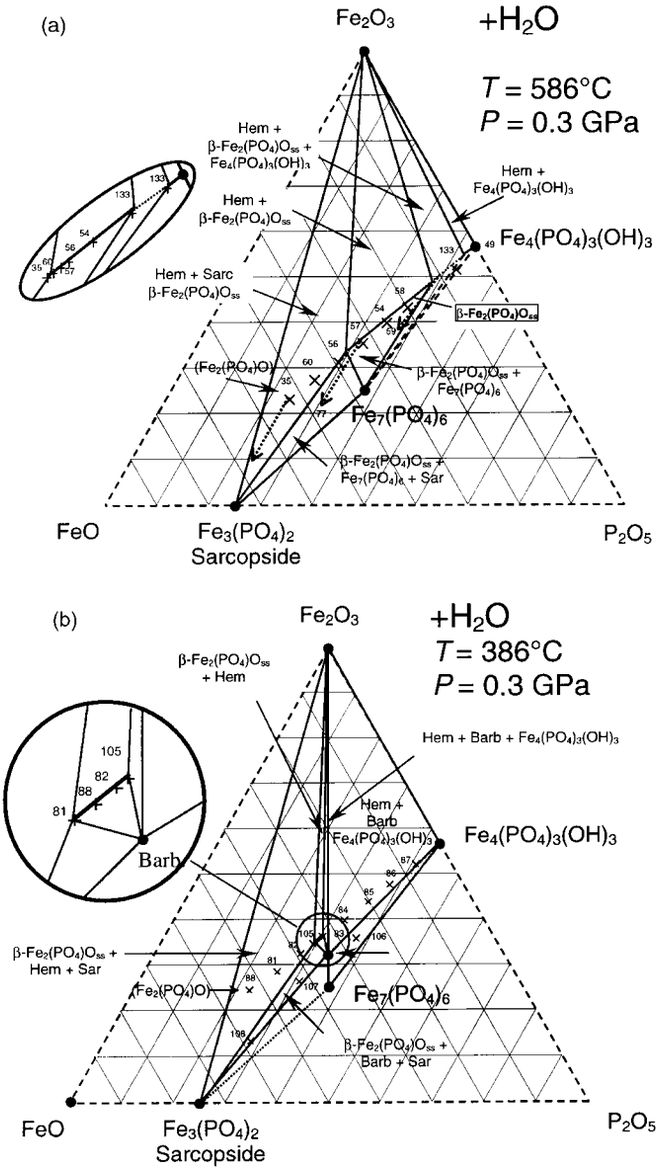

Fig. 4 The system FeO–Fe_2O_3–P_2O_5–H_2O projected onto the anhydrous base at (a) 586 and (b) 386 °C, both at 0.3 GPa. Only the phases of the quaternary subsystem Fe_2O_3–$Fe_3(PO_4)_2$–$Fe_7(PO_4)_6$–$Fe_4(PO_4)_3(OH)_3$ are shown. Diagonal crosses (×): starting bulk compositions. Vertical crosses (+): composition of the members of the β-$Fe_2(PO_4)O_{ss}$ solid solution series.

compositions of the members of the $Fe_2(PO_4)O_{ss}$ present in the samples are shown together with the numbers of the corresponding runs in the section on the left of Fig. 4b as vertical crosses (+). The members of the $Fe_2(PO_4)O_{ss}$ solid solution series were found to coexist with α-Fe_2O_3 (hematite), $Fe_3(PO_4)_2$ (sarcopside), $Fe_7(PO_4)_6$ and the now stable phase $Fe_3(PO_4)_2(OH)_2$ (barbosalite). Analogously to the runs at 586 °C the pure compound β-$Fe_2(PO_4)O$ was not formed at 386 °C. An experiment with the corresponding composition (Barb-88) leads to a phase composition of $Fe_3(PO_4)_2$ (sarcopside), α-Fe_2O_3 (hematite) and a member of the $Fe_2(PO_4)O_{ss}$ solid solution series with a compositional parameter of $x = 0.55$ (Table 4).

Towards the data point representing the ferric compound $Fe_4(PO_4)_3(OH)_3$ the join $Fe_2(PO_4)O$–$Fe_4(PO_4)_3(OH)_3$ was also found to be pseudo binary. Two 3-phase fields [hematite, barbosalite, $Fe_2(PO_4)O_{ss}$] and [hematite, barbosalite, $Fe_4(PO_4)_3(OH)_3$] were identified. Fig. 5 shows the development of the powder diffraction patterns in the latter 3-phase field. The diffractograms of the samples Barb-85, -86 and -87 can be interpreted as superpositions of the diffraction patterns of pure barbosalite (Barb-14), $Fe_4(PO_4)_3(OH)_3$ (Barb-49) and α-Fe_2O_3. In Fig. 5the decreasing and increasing reflections typical for these phases are indicated with dashed vertical lines. Additionally Fig. 5 demonstrates the constancy of the lattice properties (here the unit cell volume V) of the constituents barbosalite and $Fe_4(PO_4)_3(OH)_3$. Such a constancy of the lattice properties is required for bulk compositions in a miscibility gap as the intrinsic properties are independent of the bulk composition. Additionally the weight portions of barbosalite (Fig. 5b) derived from the diffractions *via* multiphase Rietveld refinement (Table 2) agree well with the weight portions calculated from the starting bulk compositions for coexisting barbosalite, $Fe_4(PO_4)_3(OH)_3$ and hematite.

Discussion

In a previous paper the existence of a restricted solid solution series which is located between the $Fe_2(PO_4)O$ and the $Fe_4(PO_4)_3(OH)_3$ compositions in the quaternary system FeO–Fe_2O_3–P_2O_5 was reported.[4] At 586 °C this solid solution extends over the compositional range $0.18 \leqslant x \leqslant 0.60$ (Fig. 4a). As can be seen from Fig. 4b reduction of the temperature from 586 to 386 °C strongly reduces the range of the solid solution to $0.52 \leqslant x \leqslant 0.58$

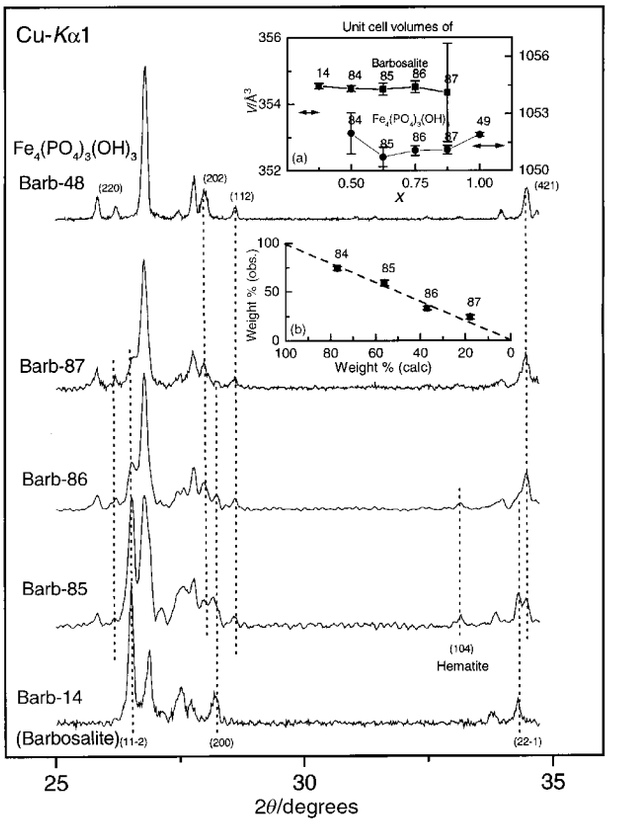

Fig. 5 Powder diffraction patterns of samples in the three phase field in the $Fe_4(PO_4)_3(OH)_3$ rich portion of the pseudo binary section between $Fe_2(PO_4)O$–$Fe_4(PO_4)_3(OH)_3$ (Fig. 4b). The samples which were synthesised at 386 °C and 0.3 GPa are consistent with variable amounts of barbosalite [$Fe_3(PO_4)_2(OH)_2$], $Fe_4(PO_4)_3(OH)_3$ and hematite (α-Fe_2O_3). The behaviour of selected individual reflections which were used for qualitative phase analysis are shown with dashed lines. Diagram (a) shows the constancy of the cell volumes of barbosalite and the $Fe_4(PO_4)_3(OH)_3$ in the different runs. In diagram (b) the calculated weight% of barbosalite assuming a 3-phase mixture of barbosalite, $Fe_4(PO_4)_3(OH)_3$ and hematite is plotted *vs.* the observed weight portion. The dashed line presents the 1 : 1 relation.

[according to a stoichiometry of $Fe^{3+}_{4-x}Fe^{2+}_{3x}(PO_4)_3(OH)_{3-3x}O_{3x}$]. At both temperatures and for bulk compositions near $Fe_2(PO_4)O$ the H_2O fluid coexists with Fe_2O_3, $Fe_3(PO_4)_2$ (sarcopside) and a member of the $Fe_2(PO_4)O_{ss}$ solid solution series. Therefore a conode face exists between the latter three phases in the quaternary system. This conode face separates the points representing the compounds $Fe_5(PO_4)_3O$ and β-$Fe_2(PO_4)O$ which are located in the anhydrous base FeO–Fe_2O_3–P_2O_5 as well as those of the (hypothetical) members of the β-$Fe_2(PO_4)O_{ss}$ solid solution series with x higher than 0.58–0.60 from the H_2O apex. This situation is visualised in Fig. 6 which is a tetrahedral representation of the quarternary system FeO–Fe_2O_3–P_2O_5–H_2O. The dashed triangle with the corners A–B–H_2O is a pseudo ternary section which includes the β-$Fe_2(PO_4)O_{ss}$ solid solution as well as the end member compositions $Fe_2(PO_4)O$ and $Fe_4(PO_4)_3(OH)_3$, respectively. There are two conode faces in the quaternary system which characterise the phase relations of β-$Fe_2(PO_4)O_{ss}$. One of them is spanned by the range of the β-$Fe_2(PO_4)O_{ss}$ solid solution itself (present in the hydrothermal run products and labelled * in Fig. 6) and the Fe_2O_3 (hematite) apex. The second triangular conode face is that between sarcopside, hematite and the limiting member of the β-$Fe_2(PO_4)O_{ss}$ solid solution series. The representative points of the compounds $Fe_2(PO_4)O$ and $Fe_5(PO_4)_3O$ are located below these two conode faces in the anhydrous base FeO–Fe_2O_3–P_2O_5(dotted triangle). Therefore no tieline can exist between these phases and the H_2O apex.

Further the bulk compositions of the hydrothermal runs which are typically characterised by an excess of H_2O are located well above the triangular conode faces near to the H_2O apex.

Consequently the compounds located below the mentioned conode faces and in the anhydrous base FeO–Fe_2O_3–P_2O_5 cannot appear in typical hydrothermal runs with excess H_2O under equilibrium conditions. Therefore it cannot principally be excluded that there is an extension of the β-$Fe_2(PO_4)O_{ss}$ solid solution series down to the β-$Fe_2(PO_4)O$ end member as drawn in Fig. 6 with a dotted line.

Catalytic experiments were performed at 385 °C and normal pressure using an initial gas flow with a total flow rate of 1 $cm^3\ s^{-1}$ and partial pressures for isobutyric acid, H_2O, O_2 and N_2 of 5.86, 72, 4.26 and 19.2 kPa at 385 °C, respectively.[3,20] It was reported that $Fe^{2+}Fe^{3+}_2(PO_4)_2(OH)_2$ as well as $Fe_{2.24}(PO_4)_3(OH)_{2.28}O_{0.72}$ and $Fe_5(PO_4)_3O_3$ changed their compositions during the catalytic runs resulting in three members of the β-$Fe_2(PO_4)O_{ss}$ solid solution series. This would give rise to a minimum compositional range between $0.12 \leqslant x \leqslant 0.50$ at 385 °C. This is in disagreement with the results of this paper as hydrothermal runs at the same temperature revealed a range of solid solutions between $0.52 \leqslant x \leqslant 0.58$. According to these authors the X-ray patterns of their Fe-hydroxyphosphates after catalysis were very similar. They corresponded to that of $Fe_4(PO_4)_3(OH)_3$ and the calculation of the cell parameters did not show any significant variations.[20] Contrasting to these observations significant variations can be detected in the lattice properties of the β-$Fe_2(PO_4)O_{ss}$ solid solution series over such a compositional range.[4] Therefore it can be argued that the samples (after catalysis) of the previously mentioned authors were multiphase mixtures with a bulk composition located in the 3-phase field like those on the right of the restricted β-$Fe_2(PO_4)O_{ss}$ solid solution series in Fig. 4b at 386 °C and 0.3 GPa.

Information concerning the phase relations in the anhydrous system FeO–Fe_2O_3–P_2O_5 can only be deduced from these hydrothermal experiments if the phases of the anhydrous base can coexist directly with the H_2O fluid. This is the case for the experiments Barb-35 and -88 where $Fe_3(PO_4)_2$ (sarcopside) and Fe_2O_3 (hematite) were identified as run products. Therefore a tieline between the latter phases is present in the phase diagrams at 386 and 586 °C and 0.3 GPa (Fig. 4). In contrast to this the phase diagram under dry conditions (Fig. 2) shows a tieline between $Fe_5(PO_4)_3O$ and Fe_3O_4 (magnetite) which excludes a coexistence of $Fe_3(PO_4)_2$ and Fe_2O_3. As these results were achieved in synthesis experiments in evacuated silica tubes at 900 °C[11] one can conclude that at a temperature between 600 °C and 900 °C the cross reaction:

$$3/2Fe_3(PO_4)_2 + Fe_2O_3 \Rightarrow Fe_5(PO_4)_3O + 1/2Fe_3O_4 \qquad (2)$$

has to take place, in the course of which the tieline between $Fe_5(PO_4)_3O$ and Fe_3O_4 (magnetite) replaces the one between Fe_2O_3 (hematite) and $Fe_3(PO_4)_2$.

The latter compound, $Fe_3(PO_4)_2$, is present in synthesis experiments at 900 °C (and very low pressures) like those of Modaressi *et al.*[11] in its high temperature modification graftonite whereas in the hydrothermal run products of this paper at 386 and 586 °C at 0.3 GPa the low temperature form[21] sarcopside was found. These latter observations are in agreement with previous hydrothermal studies on sarcopside syntheses which were performed in the pressure and temperature ranges between $0.05 \leqslant P \leqslant 0.1$ GPa and $250 \leqslant T \leqslant 650$ °C.[21–23] As hydrothermal experiments at elevated temperatures require higher pressures than syntheses in silica tubes a pressure dependency of the phase transformation sarcopside $\Leftrightarrow$ graftonite cannot be ruled out from the above mentioned results. But as the molar volumes of sarcopside ($V_m = 9.07(1)$ ml mol^{-1})[24] and graftonite

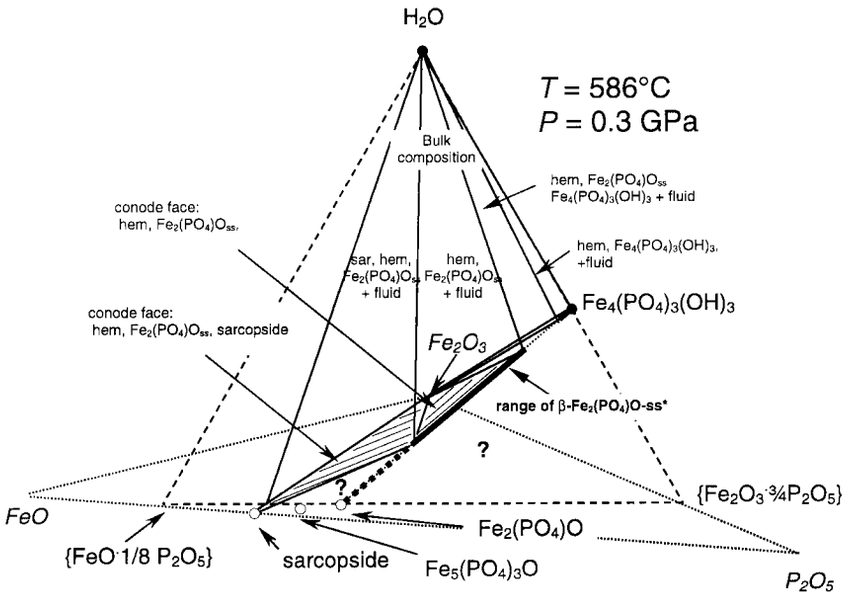

Fig. 6 Pseudo ternary section (dashed triangle) through the system FeO–Fe_2O_3–P_2O_5–H_2O along the β-$Fe_2(PO_4)O$–$Fe_4(PO_4)_3(OH)_3$ solid solution series at 586 °C and 0.3 GPa. The compositions of the corners of this section in the binary systems are given in braces {}. The bulk compositions of the hydrothermal runs (Tables 1 and 2) are located near the H_2O apex due to excess H_2O. Therefore the phase relations below the β-$Fe_2(PO_4)O_{ss}$ solid solution series and the trace of the conode face [hematite, β-$Fe_2(PO_4)O_{ss}$, sarcopside] cannot be investigated in typical hydrothermal runs with excess H_2O.

($V_m = 9.06(1)$ ml mol^{-1})[25] are nearly equal a strong influence of pressure on the univariant curve of the phase transformation in the *P–T* field is doubtful. A metastable character for sarcopside is also improbable as formation of sarcopside can be achieved from alternative starting materials like graftonite,[22,23] $Fe_3(PO_4)_2 \cdot nH_2O$[21] or a mixture of Fe, Fe_2O_3 and $FePO_4$ (this study).

Influence of different starting compounds on the synthesis of $Fe_2(PO_4)O_{ss}$

Ijjaali *et al.*[1] argued that β-$Fe_2(PO_4)O$ may have been formed metastably in their synthesis experiments. Generally it cannot be excluded that only a distinct reaction path which may be characterised by distinct starting compounds or synthesis methods results in a metastable phase whereas others would produce the stable phase agglomeration. Therefore members of the $Fe_2(PO_4)O_{ss}$ solid solution series with a chemical bulk composition corresponding to a compositional parameter $x_{start} = 0.286$ were synthesised hydrothermally from mixtures of different starting compounds. This cannot be regarded as an ultimate test for the stability or metastability of the formation of a compound as the former cannot be proved in a positive sense but it reduces the probability of the latter. The applied mixtures consisted of: $FePO_4$–Fe_2O_3–Fe, α-$Fe_2(PO)_4O + Fe_4(PO_4)_3(OH)_3$, $Fe_3(PO_4)_2 + Fe_2O_3 + FePO_4$ and $[Fe_3(PO_4)_2 + Fe_2O_3 + Fe_7(PO_4)_6\} + \{Fe_7(PO_4)_6 + Fe_2O_3 + FePO_4]$

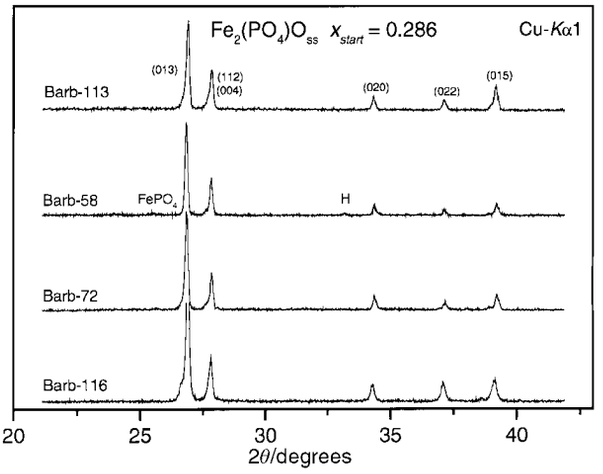

Fig. 7 X-Ray powder diffraction patterns of samples synthesised from different starting mixtures at 586 °C and 0.3 GPa . Each run yielded a member of the β-$Fe_2(PO_4)O_{ss}$ solid solution series revealing that their formation is independent of the starting material under these conditions. Abbreviations: H: hematite (α-Fe_2O_3).

These starting mixtures were subjected to reaction conditions of 586 °C and 0.3 GPa over a reaction period of 2 to 3 days under water saturated conditions (Table 3). A section of the powder diffractograms of these samples is given in Fig. 7. In each experiment the run products consisted of a nearly phase pure member of the $Fe_2(PO_4)O_{ss}$ solid solution series. Only in the case of sample Barb-58 were small amounts of hematite and $FePO_4$, which were among the starting compounds, found to be present. Their presence can therefore easily be interpreted as due to an incomplete reaction. The compositional parameters *x* of the $Fe_2(PO_4)O_{ss}$ solid solution members calculated with the calibration curve from eqn. (1) can be taken from Table 4. These parameters scatter around the value of the starting mixture $x_{start} = 0.286$. Nevertheless in each case a member of the $Fe_2(PO_4)O_{ss}$ solid solution series was formed. The above mentioned scattering of the determined compositions can be explained by a different degree of oxidation of the charges due to the influence of the outer pressure medium. Therefore these results support the assumption that the $Fe_2(PO_4)O_{ss}$ solid solution is a stable product under the applied hydrothermal conditions.

Conclusions

In hydrothermal synthesis experiments under H_2O saturated conditions at 386 and 586 °C and 0.3 GPa the phase relations of the restricted β-$Fe_2(PO_4)O_{ss}$ solid solution series in the quaternary system FeO–Fe_2O_3–P_2O_5–H_2O were clarified. On reducing the temperature from 586 to 386 °C the compositional range of this solid solution series, which is stable with excess of H_2O, is reduced from $0.18 \leqslant x \leqslant 0.60$ to $0.52 \leqslant x \leqslant 0.58$ with respect to a stoichiometry of $Fe^{3+}_{4-x}Fe^{2+}_{3x}(PO_4)_3(OH)_{3-3x}O_{3x}$ (Fig. 4). From the hydrous mineral phases shown in Fig. 3 only barbosalite [$Fe_3(PO_4)_2(OH)_2$] was found to be present in the

run products (at 386 °C). The mineral wolfeite $Fe_2(PO_4)OH$ might be stable under these elevated temperatures due to its low H_2O content. But as its compositional data point is located on the left side of the conode face between $Fe_3(PO_4)_2$, Fe_2O_3 and H_2O outside the investigated area of Fig. 4 it could not be detected in the run products. Neither pure $Fe_2(PO_4)O$, in its α- or β-form, nor the compound $Fe_5(PO_4)_3O$ were found to coexist with the H_2O bearing fluid phase under the applied conditions. This can be explained by the observation that their representive data points in the quaternary system $FeO–Fe_2O_3–P_2O_5–H_2O$ are separated from the H_2O apex by a conode face which is spanned by the three phases $Fe_3(PO_4)_2$ (sarcopside), α-Fe_2O_3 (hematite) and a member of the $Fe_2(PO_4)O_{ss}$ solid solution series (Figs. 4a and b). Therefore it cannot be excluded that $Fe_2(PO_4)O$ and $Fe_5(PO_4)_3O_3$ are stable under these *P–T* conditions but lower H_2O-fugacities, an aspect which must be left to further investigation.

Acknowledgements

The author thanks Professor L. Cemič for critical reading of the manuscript. This investigation was financially supported by the Deutsche Forschungsgemeinschaft (Project no. Schm 932/3-1)

References

1 M. Ijjaali, B. Malaman, C. Gleitzer, K. Warner, J. A. Hriljac and A. K. Cheetham, *J. Solid State Chem.*, 1990, **86**, 195.
2 J. M. M. Millet, *Catal. Rev. Sci. Eng.*, 1998, **40**, 1.
3 D. Rouzies, J. M. M. Millet, D. S. H. Sam and J. C. Védrine, *Appl. Catal. A*, 1995, **124**, 189.
4 P. Schmid-Beurmann, *J. Solid State Chem.*, 2000, **153**, 239.
5 C. Virely, M. Forissier, J.-M. M. Millet, J. C. Védrine and D. Huchette, *J. Mol. Catal.*, 1992, **71**, 199.
6 B. Ech-Chahed, F. Jeannot, B. Malaman and C. Gleitzer, *J. Solid State Chem.*, 1988, **74**, 47.
7 E. Elkaïm, J. F. Berar, C. Gleitzer, B. Malaman, M. Ijjaali and C. Lecomte, *Acta Crystallogr., Sect. B*, 1996, **52**, 428.
8 A. Modaressi, A. Courtois, R. Gerardin, B. Malaman and C. Gleitzer, *J. Solid State Chem.*, 1981, **40**, 301.
9 Y. Gorbunov, B. Maksimov, Y. Kabalov, A. Ivachenk, O. Melnikov and N. Belov, *Dokl. Akad. Nauk SSSR (Engl. Transl.)*, 1980, **25**, 785.
10 A. Moguš-Milanković, M. Rajić, A. Drašner, R. Trojko and D. E. Day, *Phys. Chem. Glasses*, 1998, **39**, 70.
11 A. Modaressi, J. C. Kaell, B. Malaman, R. Gérardin and C. Gleitzer, *Mater. Res. Bull.*, 1983, **18**, 101.
12 C. C. Torardi, W. M. Reiff and L. Takaks, *J. Solid State Chem.*, 1989, **82**, 203.
13 M. Ijjaali, B. Malaman, C. Gleitzer and M. Pichavant, *Eur. J. Solid State Inorg. Chem.*, 1989, **26**, 73.
14 J. Korinth and P. Royen, *Z. Anorg. Allg. Chem.*, 1961, **313**, 121.
15 C. L. Lengauer, HILL, Institut für Mineralogie, Kristallographie und Strukturchemie der Universität Wien, Wien, 1993.
16 R. L. Blake, R. E. Hessewick, T. Zoltai and L. W. Finger, *Am. Mineral.*, 1966, **51**, 123.
17 P. B. Moore, *Am. Mineral.*, 1972, **57**, 24.
18 G. Giuseppetti and C. Tadini, *Neues Jahrb. Mineral. Monatsh.*, 1983, **9**, 410.
19 J. S. Huebner, in *Research Techniques for High Temperature and High Pressure*, ed. G. C. Ulmer, Springer Verlag, Berlin, Heidelberg, New York, 1971, p. 123.
20 J.-M. M. Millet, D. Rouzies and J. C. Védrine, *Appl. Catal. A*, 1995, **124**, 205.
21 E. Mattievich and J. Danon, *J. Inorg. Nucl. Chem.*, 1977, **39**, 569.
22 T. Ericsson and A. G. Nord, *Am. Mineral.*, 1984, **69**, 889.
23 G. Charalampides, T. Ericsson, A. G. Nord and F. Khangi, *Neues Jahrb. Mineral. Monatsh.*, 1988, **H7**, 324.
24 T. Ericsson, A. G. Nord and G. Åberg, *Am. Mineral.*, 1986, **71**, 136.
25 E. Kostiner and J. R. Rea, *Inorg. Chem.*, 1974, **13**, 2876.
26 D. Rouzies and J. M. M. Millet, *Hyperfine Interact.*, 1993, **77**, 11.
27 P. Ramdohr and H. Strunz, *Lehrbuch der Mineralogie*, Enke Verlag, Stuttgart, 1978.
28 *DIFFRAC-AT*, ver. 3.0, Firma Siemens, Karlsruhe, 1991.